ISSN 1674-1056
http://cpb.iphy.ac.cn
http://iopscience.iop.org/cpb
中国物理 B
Chinese Physics
中国物理 Chinese Physics B

Monitoring the formation of oil-water emulsions with a fast spatially resolved NMR spectroscopy method

Meng-Ting You(游梦婷), Zhi-Liang Wei(韦芝良), Jian Yang(杨健), Xiao-Hong Cui(崔晓红), Zhong Chen(陈 忠)
Citation: Chin. Phys. B . 2018, 27(2): 028201. **doi:** 10.1088/1674-1056/27/2/028201

Journal homepage: http://cpb.iphy.ac.cn; http://iopscience.iop.org/cpb

What follows is a list of articles you may be interested in

Hydrodynamics of passing-over motion during binary droplet collision in shear flow

Cheng-Yao Wang(王程遥), Cheng-Bin Zhang(张程宾), Xiang-Yong Huang(黄庠永), Xiang-Dong Liu(刘向东), Yong-Ping Chen(陈永平)
Chin. Phys. B . 2016, 25(10): 108202. **doi:** 10.1088/1674-1056/25/10/108202

A new solvent suppression method via radiation damping effect

Cui Xiao-Hong, Peng Ling, Zhang Zhen-Min, Cai Shu-Hui, Chen Zhong
Chin. Phys. B . 2011, 20(11): 118201. **doi:** 10.1088/1674-1056/20/11/118201

SPECIAL TOPIC — Soft matter and biological physics

Monitoring the formation of oil–water emulsions with a fast spatially resolved NMR spectroscopy method*

Meng-Ting You(游梦婷)[1], Zhi-Liang Wei(韦芝良)[1,2], Jian Yang(杨健)[1], Xiao-Hong Cui(崔晓红)[1,†] and Zhong Chen(陈忠)[1]

[1] Department of Electronic Science, State Key Laboratory of Physical Chemistry of Solid Surfaces, Xiamen University, Xiamen 361005, China
[2] Department of Radiology, The Johns Hopkins University, Maryland, USA

(Received 6 August 2017; revised manuscript received 1 December 2017; published online 5 January 2018)

In the present study, a fast chemical shift imaging (CSI) method has been used to dynamically monitor the formation of oil–water emulsions and the phase separation process of the emulsion phase from the excessive water or oil phase on the molecular level. With signals sampled from series of small voxels simultaneously within a few seconds, high-resolution one-dimensional (1D) ^{1}H nuclear magnetic resonance (NMR) spectra from different spatial positions for inhomogeneous emulsion systems induced by susceptibility differences among components can be obtained independently. On the basis of integrals from these ^{1}H NMR spectra, profiles obtained explicitly demonstrate the spatial and temporal variations of oil concentrations. Furthermore, the phase separation time and the length of the oil–water emulsion phase are determined. In addition, effects of oil types and proportions of the emulsifier on the emulsification states are also inspected. Experimental results indicate that 1D PHASICS (Partial Homogeneity Assisted Inhomogeneity Correction Spectroscopy) provides a helpful and promising alternative to research on dynamic processes or chemical reactions.

Keywords: non-invasive monitoring, spatially-resolved NMR spectroscopy, formation of emulsions, phase separation process

PACS: 82.56.–b, 76.60.–k, 82.70.Kj **DOI:** 10.1088/1674-1056/27/2/028201

1. Introduction

Emulsions are metastable colloids made out of two immiscible fluids, one being dispersed in the other, in the presence of surface active agents. Due to advantages in enhancing the solubility and bioactivity of lipophilic ingredients, O/W emulsions have been widely used in various fields, including food,[1–3] cosmetics,[4–6] and pharmaceutical industries.[7–9] The knowledge of the formation mechanism of emulsions has great significance in understanding the stability of emulsions and phase separation progress. Traditional methods to evaluate structures and dynamics of emulsions include light-scattering,[10,11] microscopy,[12] conductivity measurements,[13] and rheological technique,[14,15] etc., which provide information including droplet size distribution (DSD), morphology, stability, and rheology of emulsions. Nuclear magnetic resonance (NMR) spectroscopy has long been served as a powerful and versatile method for molecular-level analyses of chemicals and biological metabolites in various fields.[16–18] With respect to emulsions, NMR offers a non-invasive ability to measure the emulsion DSD via quantifying molecular self-diffusion using pulsed field gradients (PFG) techniques, which is able to handle very concentrated emulsions whose sizing is generally beyond the capability of other alternative methods.[19] Except for the DSD measurement, proton NMR (^{1}H NMR) has been used to identify and quantify oxidation products in oil-in-water emulsion during storage.[20] Another study has also demonstrated the usefulness of magnetic resonance (MR) techniques, including MR imaging (MRI)[21] and MR spectroscopy (MRS) for non-destructive monitoring of creaming of oil-in-water emulsion-based formulations.[22]

Recently, a novel approach based on volume-selective NMR spectroscopy which induces no mechanical perturbation of the interface was used to obtain spatially resolved one-dimensional (1D) NMR spectroscopy for the system water–benzene.[23] With the high strength of the field gradient along the Z direction up to 1 T·m^{-1}, a detection volume thickness of 1 μm and the shift increment of 50 nm provide the possibility for the investigation of liquid–liquid interfaces at high spatial resolution. However, basic probes that equip most liquid-state NMR spectrometers are direct or indirect detection probes, with the field gradient along the Z axis only for the selection of coherence pathways and measurement of self-diffusion coefficients. Therefore, a number of methods that can be easily implemented on the standard solution NMR equipment found in chemistry laboratories have been proposed for generating slice-resolved spectra of biphasic systems prepared in conven-

*Project supported by the Natural Science Foundation of Fujian Province, China (Grant Nos. 2016J01078 and 2017J05011), the Fundamental Research Funds for the Central Universities of China (Grant Nos. 20720160125 and 20720150018), and the National Natural Science Foundation of China (Grant No. 11705068).

†Corresponding author. E-mail: cuixh@xmu.edu.cn

© 2018 Chinese Physical Society and IOP Publishing Ltd

tional NMR tubes, thus ensuring a wide application to various chemical systems.[24,25] Recently, a method based on partial homogeneity termed as PHASICS (Partial Homogeneity Assisted Inhomogeneity Correction Spectroscopy) was proposed for retrieving high-resolution NMR spectroscopy[26] under inhomogeneous fields with the aid of pattern recognition. Signals from series of small voxels, which characterize high-resolution due to small sizes, are recorded simultaneously. With an echo planar spectroscopic imaging (EPSI) detection module, high resolution 1D ^{1}H NMR spectra can be simultaneously recorded by PHASICS both with the chemical shift and spatial information within a few seconds.[27] Compared to single-voxel MRS, multi-voxel spectral information covering the whole effective sample length along the gradient orientation can be accomplished simultaneously with the utilization of frequency-encoding gradients during the acquisition period at high slew rate.

To date, preparations and properties of emulsions including the stability,[28–30] solubility,[31–33] and so forth have aroused many concerns and been investigated by aforementioned traditional techniques. However, to the best of our knowledge, current reports have not exposed the formation process of the oil–water emulsion by NMR spectroscopy at a molecular level. Due to the susceptibility difference at the interface between oil and water, the magnetic field inside the emulsion system is inhomogeneous. Furthermore, the magnetic field is also unstable, because of the dynamic emulsification reactions during the emulsion stabilization. Therefore, in this study, the feasibility of quantitative analyses with high-resolution spatially-resolved PHASICS pulse sequence is explored by dealing with the basic emulsification process between water and oil in the presence of an emulsifier. Typically, poloxamer 188 was chosen as the emulsifier, which is a kind of nonionic surfactant and broadly evaluated for various drug delivery applications as an O/W emulsifier. Besides, in order to monitor the spatial migration of different components for emulsified systems from being mixed to stratified, equal volumes of oil and water were used to prepare emulsions. In addition, effects of proportions of poloxamer 188 on the thicknesses of emulsions and phase separation times were further examined.

2. Materials and Methods

2.1. Materials

Sesame oil and corn oil were purchased from a local supermarket and used directly without any pretreatment. Poloxamer 188 was purchased from a local chemical products retailer (Jilin GmbH, Xiamen, China) and used directly without further purification. D_2O (99.8%) and $CDCl_3$ (99.8%) are the product of Norell (USA). D_2O and distilled water were used to prepare emulsions.

2.2. Emulsion preparation

Initially, an aqueous emulsifier solution was prepared by dispersing poloxamer 188 in the aqueous phase and spun with a vortex at room temperature to ensure complete dissolution. Two proportions of poloxamer 188 of 0.35 g/L and 0.70 g/L were chosen to investigate effects of different amounts of the emulsifier on the emulsion formation. In order to avoid the potential radiation damping effect, the aqueous phase consisted of 10% (v/v) H_2O and 90% (v/v) D_2O. Emulsions were prepared by blending equal volumes of the organic phase (sesame oil or corn oil) and the aqueous emulsifier solution, and then spun with a vortex for 5 min at room temperature.

In order to test the feasibility of spatially resolved spectroscopy of PHASICS in biphasic systems, a verification experiment was performed using a sample consisting of two immiscible fluids: D_2O as the aqueous phase, and sesame oil (diluted with $CDCl_3$ in the volume ratio of 1:10) as the oil phase.

2.3. Methods

The PHASICS method was proposed for obtaining high-resolution 1D NMR spectra by recording signals from different voxels independently and reconstructing high-resolution spectra with the inhomogeneity correction algorithm. The entire sequence starts with an excitation pulse, followed by two blocks of phase encoding along the X and Y axes, and ends in an echo planar spectroscopic imaging (EPSI) detection module to simultaneously record both the chemical shift information and the spatial information. Phase encoding modules in PHASICS are optional in practical applications. Without phase encoding modules along the X and Y axes, PHASICS is capable of obtaining high-resolution spectra under the inhomogeneity along the Z axis, termed as 1D PHASICS (Fig. 1). The brief description about 1D PHASICS is given as follows. All spins in the sample are excited by the 90° pulse; because of the existence of frequency-encoding gradient Ga along the Z direction, spins with different Z positions possess different phase information, achieving the spatial localization along the Z direction. Chemical shift information can be obtained by repeating EPSI module. The $+G_a$ and $-G_a$ gradients represent reverse frequency-encoding directions. Under such gradients, data acquired in odd and even lobes construct two sets of k-space which should be processed separately. These two processed data sets contain in principle the identical spectral and spatial information. In this study, only $+G_a$ data sets are employed saving the trouble of subsequent phase-correction and combination of two data sets. G_S is the compensation gradient to adjust positions of echo centers. The single-scan nature of 1D PHASICS can be valuable when we attempt to analyze chemical reactions or dynamic processes within NMR tubes. It has been elaborated that the resolution will be improved with

the decrease of the voxel size by PHASICS under inhomogeneous fields.[25] However, intensities of frequency-encoding gradients must be enlarged for selecting smaller voxels. Meanwhile, the receiver bandwidth must be further magnified to accommodate increased gradients, however, more noise is introduced. As a result, the signal-to-noise ratio (SNR) performance deteriorates. As the reference indicated, in practical applications, PHASICS experiments can be carried out with suitable parameters to reach a compromise among resolution, acquisition time, and SNR.[27]

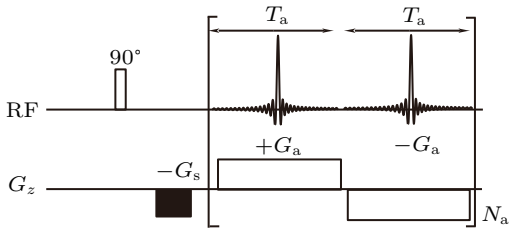


Fig. 1. 1D PHASICS pulse sequence. The open rectangle on the RF axis represents the 90° nonselective pulse; G_a the frequency-encoding gradient; T_a the duration of encoding gradient with single polarity; N_a the total number of bipolar encoding gradients; G_S the compensation gradient to adjust positions of echo centers.

Optimized experimental parameters for the verification experiment were: spectral width (SW) 500 kHz, intensities of frequency-encoding gradients during the acquisition period (G_a) 36.6 Gs/cm (1 Gs = 10^{-4} T), the duration of each single gradient lobe (T_a) 160 μs, the number of pairs of frequency-encoding gradients, i.e., repetition times of the detection block (N_a) 600, number of sampling points during the duration of T_a (N_{p1}) 80, without signal average. The pulse repetition time was set as 3 s, and the total experiment time 4 s. Emulsion experiments shared most experimental parameters in the verification experiment, except the scanning number was equal to 16. According to experimental parameters, the interval of sampling points ($\Delta\tau$) can be figured out as 2 μs (reciprocal of spectral width), the effective sample length (L) can be calculated as 32 mm by

$$L = 1/(\gamma G_a \Delta\tau). \tag{1}$$

The spatial resolution can be calculated as 0.40 mm by

$$\Delta z = L/Np_1. \tag{2}$$

The above equations indicate that each 1D NMR spectrum extracted from the two-dimensional (2D) map provides the information of each sample voxel with a thickness of 0.40 mm. The raw data obtained from PHASICS protocols were processed using in-house programs based on MATLAB.

The process of reconstructing high-resolution spectra includes the rearrangement process and correction algorithm. The rearrangement process is implemented as follows: first, rearrange the raw data from PHASICS to a 2D matrix. In this experiment, each acquisition under each gradient lobe contains full spatial information, which can be assigned as one row of the 2D matrix. Chemical shift information obtained by the repetition of the detection block is written as another row of the matrix. Second, apply the 2D Fourier transform to the 2D matrix. 2D maps stacked by series of 1D spectrum from different positions can be obtained. In order to remove frequency offsets induced by field inhomogeneity, the inhomogeneity correction algorithm based on pattern recognition is implemented as figure 2 shows. First, extract the PHASICS as an image and binarize the image to obtain matrix M; second, apply the component extraction to connect adjacent elements and offer a new matrix M_0; third, apply the contour extraction operation to M_0 for extracting different parts corresponding to different resonances; and finally, calculate the central-line coordinates based on the extracted contour to serve as the correction information and apply circular shifting to the original PHASICS according to the obtained correction information.[27] In this study, all the raw data from PHASICS were processed according to the above-mentioned rearrangement process. However, the correction algorithm was only applied to the biphasic sample but not emulsion samples. There are two reasons for this. Firstly, for emulsion samples, quantitative analyses are based on 1D ^{1}H NMR spectra, which characterize high-resolution due to small voxel sizes and would not be improved by the correction algorithm. Secondly, in general, the correction algorithm works well on the condition that the system has a dominant component. However, for emulsion systems there are varying contents of water and oil. It may lead to certain performance degenerations by tracking the behavior of field inhomogeneity via a single resonance.

It has been discussed that fluctuations parallel to the interfacial surface will be slow on NMR timescales and hence can be ignored.[23] In our experiments, due to the increasing of viscosity and big particle size for emulsion systems, diffusion will be slower and can be ignored within the small width of voxel. Besides, effects of gradients on the longitudinal relaxation can also be ignored, since gradients mainly affect the transverse magnetization. Although the transverse relaxation would probably be altered under gradients, reliable relative quantification results obtained with the same experimental parameters can be expected in contrast experiments. In addition, it is noteworthy that 1D spectra obtained by PHASICS cannot be phase-corrected at the same time and must be displayed in amplitude mode due to the sampling mode of EPSI. In this case, in amplitude displayed spectrum, resonances would be widened to some extent, resulting in the difficulty in definition of integral ranges and possibly inaccurate quantitative analysis. In order to overcome it, a program based on MATLAB for peak pattern fitting was written. The standard peak pat-

tern Gaussian function was chosen as the appropriate function to fit by comparing fitting errors with Gaussian and Lorentz functions. Then, by fitting the resonance of methyl protons (1.30 ppm) from oil with Gaussian function, the single peak curve can be drawn. Then, integrating the fitted curve, quantitative analysis based on integral data can be performed.

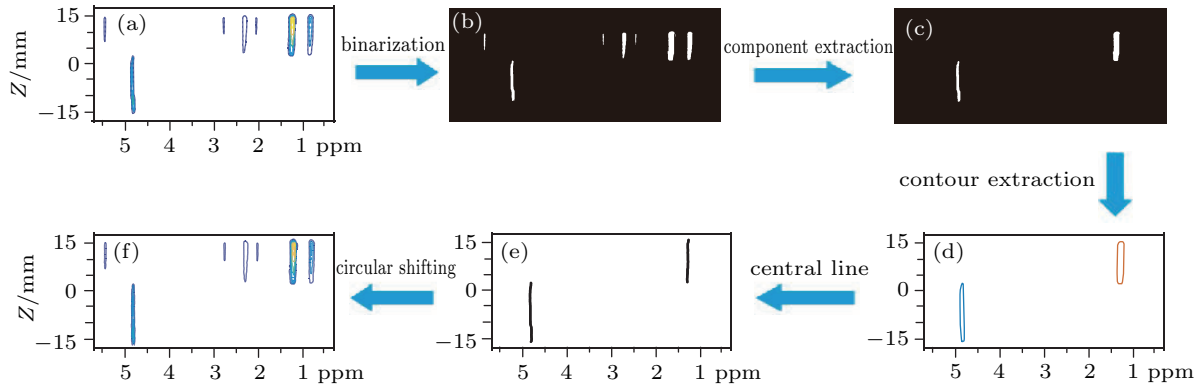


Fig. 2. (color online) Graphical representation of the correction algorithm. The biphasic sample tested under Z inhomogeneity. (a) Original spectrum by PHASICS, (b) binarized image of panel (a), (c) image after component extraction operation on panel (b), (d) extracted contours, (e) central lines calculated from contours, (f) the result after correction.

2.4. NMR measurements

NMR experiments were performed at 298 K on a 500-MHz Agilent NMR system (Agilent Technologies, Santa Clara, CA, USA) with 54-mm narrow bore, using a 5-mm switchable broadband probe together with the Z-axis pulsed field gradient. For the biphasic sample, PHASICS experiment was conducted after manually shimming magnetic field. For emulsion experiments, the sample was packed into a 5-mm NMR tube and injected into the spectrometer quickly after shaking. Because of dynamic changes during the phase separation process, the magnetic field would suffer from certain temporal variations, which were hardly removed with the shimming procedure. Therefore, before emulsion tests, a steady reference sample was adopted to provide a relatively homogeneous field. A single set of PHASICS experiment with 16 repetitions takes 1 min, and 120 PHASICS sets were successively performed covering a temporal range of 120 min in total to real-time monitor the dynamic phase separation process without shimming and locking. After data processing, appropriate data sets were chosen to build concentration profiles as required.

3. Results and discussion

3.1. Biphasic sample

Figure 3(a) present the original 2D map for D_2O and diluted sesame oil biphasic system by PHASICS. As mentioned before, with the existence of frequency-encoding gradient G_a along the Z direction, spins with different Z positions possess different phase information, achieving the differentiation of the spatial positions along the Z direction. Chemical shift information can be obtained by processing the repeating EPSI module with Fourier transform. In other words, the spectral information at different spatial positions along the Z direction (i.e., the vertical direction of the NMR tube) can be obtained separately, in which the spatial resolution depends on the strength of the encoding gradient G_a. The obtained 2D map by 1D PHASICS can be considered as a stack of series of 1D spectrum along the Z direction.

For Fig. 3(a), the sample is composed of two incompatible phases, D_2O and the diluted oil. We can find that the bottom half of the 2D contours map contains the signal from the residual water in D_2O, whereas the upper half shows different oil resonances. Although the viscosity of the sesame oil is significantly reduced after being diluted by ten times with $CDCl_3$, manual shimming still cannot lead to satisfactory results due to the magnetic susceptibility difference at the interface between two phases. Specifically, the same resonances along the Z axis are not aligned to a straight line, but shaped as two inverse crescents in 2D maps for water and oil signals. Due to the EPSI detection module, the 2D map obtained by 1D PHASICS can be considered as the magnetic field map of the sample along the Z axis. After processing by the correction algorithm, a better aligned result is obtained (Fig. 3(b)). However, for extracted 1D ^{1}H NMR, the spectral resolution which only depends on the homogeneity within the small voxel cannot be improved through the correction algorithm. Nevertheless, since the method is based on partial homogeneity, ^{1}H NMR spectra extracted from oil and water phases are intrinsically characterized by high-resolution even in the presence of field inhomogeneity (Fig. 3(c)). Corresponding integrals of methylene protons of oil and water from voxels in the most homogeneous detection area of the NMR probe with the total length of 16 mm have been portrayed into a plot of concentration versus position (z) and the interval between two adjacent

points, i.e., the spatial resolution is 0.40 mm (Fig. 3(d)). From the concentration figure, it can be found that in oil phase, oil concentrations for most positions away from the interface are strong and almost constant. However, those of water are quite low and can be considered as zero, and *vice versa*. This indicates there are no "tailing" signals from one phase to another. When approaching the interface, concentrations of both oil and water signals decrease and drop to the lowest at the center of the interface. Actually, such a componential transient process from one phase to another is quite normal, however, the range of which is expanded to some extent. The signal intensity decline over a wide range of positions is probably caused by the inhomogeneity of magnetic susceptibility near the interface. Overall, with the high spectral and spatial resolution, this experiment clearly demonstrates the feasibility of spatially resolved spectroscopy of 1D PHASICS in the biphasic system and reliable quantitative results can be derived. Coupled with single-scan acquisition traits of 1D PHASICS, it is prospected for monitoring spatial and temporal variations of the componential concentration in multiphasic systems.

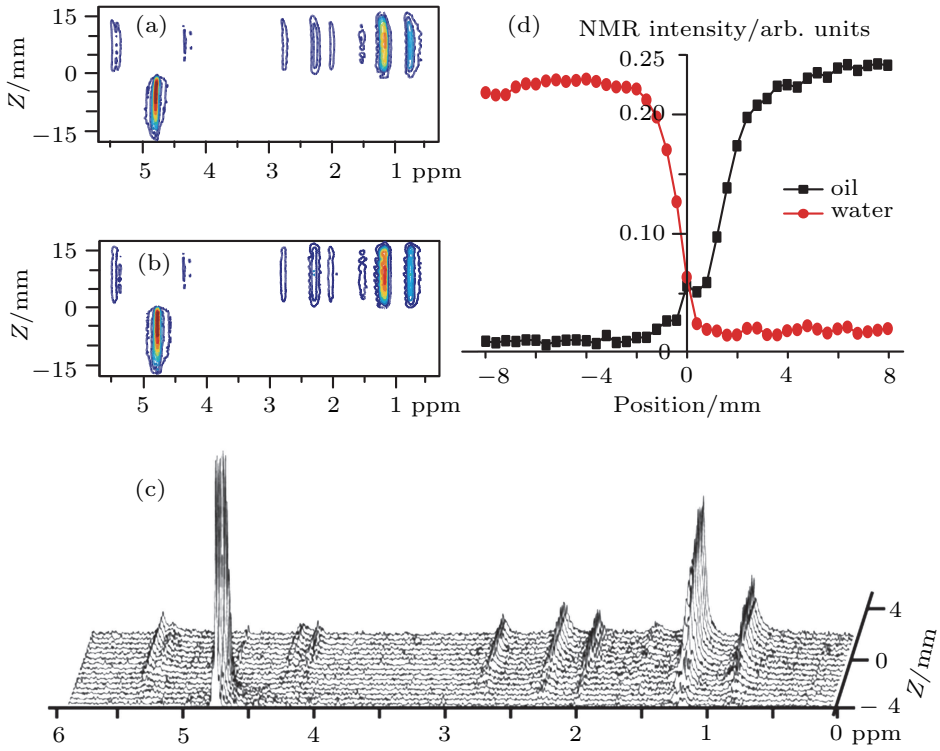


Fig. 3. (color online) Experimental results of D_2O/sesame oil biphasic system by PHASICS. Sesame oil was diluted by $CDCl_3$ with the ratio of 1:10. (a) and (b) the original and corrected 2D chemical shift contours, respectively, (c) 1D spectra extracted from 2D map with the position from 4 mm to −4 mm, (d) concentration profiles of residual water for D_2O and oil versus position (Z), respectively. The interval between two adjacent points, i.e., the spatial resolution is 0.40 mm.

3.2. Sesame oil–water emulsions

Experimental results of sesame oil–water emulsions with 0.35 g/L and 0.70 g/L of poloxamer 188 are shown in Figs. 4 and 5, respectively. Similar to the biphasic D_2O/diluted oil system, bottom halves of the 2D contour maps contain water signals and the uppers show oil resonances, respectively. However, in the middle parts it can be found that there are both water and oil signals. Combined with sample photos taken after 120 min in Figs. 4(b) and 5(b), we can observe that both samples are divided into three different phases, including transparent oil phase at the top, opaque milky oil–water emulsion phase in the middle, and aqueous phase at the bottom. These indicate that there are not only emulsion phases generated, but also excessive oil and water phases have been separated from emulsion phases. Several extracted 1D NMR spectra also demonstrate the decreasing of oil intensity along with the increasing of water intensity from top to bottom (Fig. 4(c)). However, the length of emulsion phase cannot be directly obtained from sample appearances or spectra due to ambiguous boundaries among the oil phase, oil–water emulsion phase, and aqueous phase.

Similarly, series of 2D maps for sesame oil–water emulsion systems at different times have been processed. In the same way, evolutions of 40 sesame oil concentration profiles from different voxels versus time have been portrayed and numbered as 1 to 40 from top to bottom (Figure 4(e)). Initially, oil concentrations for all profiles are very close, which indicate that the sample is mixed completely and all componential contents are very similar for different spatial voxels. From then on, oil concentration profiles gradually separate.

For the minority at the top, oil concentrations increase remarkably; those in the middle increase slowly; for the majority at the bottom, oil concentrations are rising up slightly. At 40 min, oil concentration differences between upper and lower profiles almost reach the maximum. After that, oil concentrations for upper and middle parts have kept a slowly rising trend until 120 min. Evolutions of these oil concentration profiles clearly demonstrate variations of oil concentrations at different spatial positions with the system from being mixed to the phase separation as the corresponding physical appearances shown in Fig. 4(d). For Fig. 5(c), it presents a similar trend as that of Fig. 4(e). But the distinct differentiation of profiles between the upper part and the lower part shows up at 30 min, which is earlier than that in Fig. 4(e), showing a faster process.

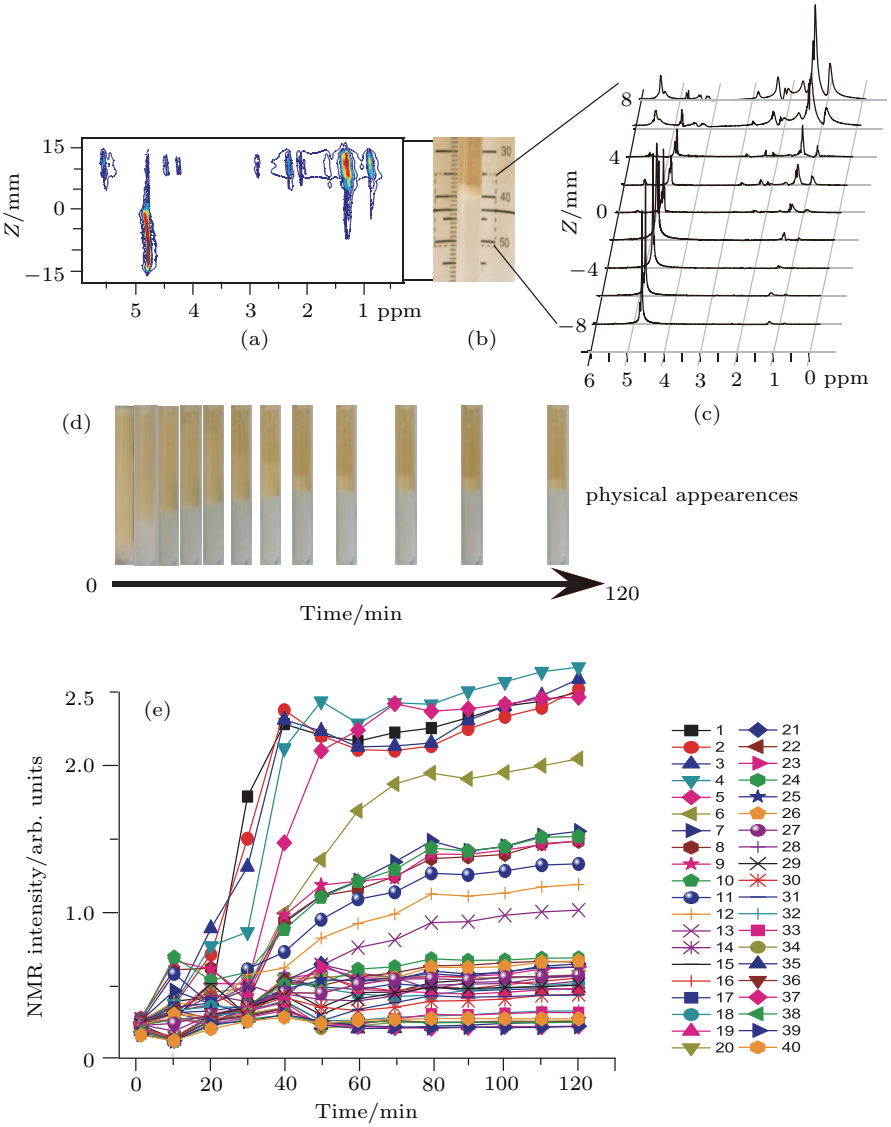


Fig. 4. (color online) Experimental results of sesame oil–water emulsion with 0.35 g/L of poloxamer 188. (a) 2D chemical shift contours, (b) sample picture after 120 min, (c) 1D spectra extracted from 2D map, (d) physical appearances, (e) sesame oil concentration profiles versus time. Concentration profiles at different spatial positions are numerically denoted as 1 to 40 from top to bottom. The spatial resolution is also 0.40 mm/profile.

After carefully examining oil profiles in Fig. 4(e), there are five profiles with high oil concentrations overlapped with each other at the top of the graph, which indicate that their oil concentrations are very similar. It can be concluded that these profiles are from those voxels located in the same phase, i.e., oil phase. Likewise, there are another two overlapped-profile regions located in the middle and at the bottom, which are assigned to another two phases present in the sample photo, i.e., the oil–water emulsion phase, and aqueous phase. Except for three overlapped-profile regions, there are 4 profiles located among them, namely, in the transient state or at interfaces between two adjacent phases. Since their oil concentrations are different from those of the oil or aqueous phase, these 4 profiles in the transition state are also assigned to the oil–water emulsion phase. With the additional 4 overlapped-profiles in the middle, according to the spatial resolution 0.40 mm, the length of the oil–water emulsion phase takes 3.2 mm.

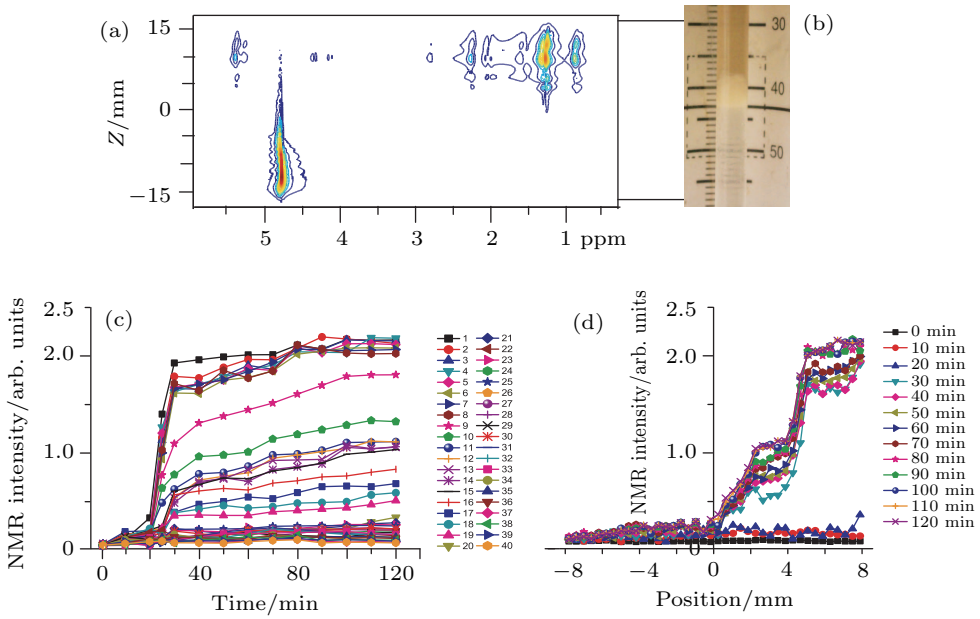


Fig. 5. (color online) Sesame oil–water emulsion with 0.70 g/L of poloxamer 188. (a) 2D chemical shift contours, (b) sample picture after 120 min, (c) and (d) sesame oil concentration profiles versus time and position, respectively.

Further comparing 2D maps and photos in Figs. 4 and 5, respectively, with the emulsifier proportion increasing, the aqueous phase length becomes shorter. Besides, three overlapped-profile regions are also assigned to oil phase, emulsion phase and aqueous phase from top to bottom, respectively (Fig. 5(c)). More concretely, there are 5 overlapped-profiles in the middle and 6 profiles in the transient state. According to the same protocol, the length of emulsion phase can be calculated as 4.4 mm which is longer than that of 3.2 mm in Fig. 4(e). From another point of view, the plot of concentration versus position (z) is also shown in Fig. 5(d). Thereinto, these points eventually gather into three parts with different oil concentrations, which corresponds to three mentioned phases, respectively. According to the positional information of the horizontal axis, a consistent emulsion phase thickness the same as Fig. 5(c) can be easily read out. As a complementary proof, both sample photos also exhibit similar results. It can be speculated that residual sesame oil and water with the additional emulsifier produce a greater amount of emulsion. Furthermore, as the amount of emulsifier increases, the phase separation time reduces. Thus, it can be speculated that the thicker the emulsion phase is, the faster it separates from water and oil phases.

Besides, in Fig. 4(e), the emerged oil concentration increases with time for all parts of the sample should be noticed. The same as the signal intensity decreases near the interface for biphasic sample, oil concentrations for all positions are very low from the initial moment to the beginning of phase separation. Since the sample is in a mixed state, the tremendous inhomogeneity of magnetic susceptibilities among components with different sizes and properties leads to the decrease of SNR and the abnormally low oil concentrations. The extremely low oil concentrations at initial moments result in apparent slight increases of oil signals in aqueous phases both for Figs. 4(e) and 5(c). As for oil increases in the oil phase and emulsion phase in Fig. 4(e), we consider that the relatively-stable phase separation has not been achieved within 120 min. For Fig. 5(c), oil concentrations in oil and emulsion phases can be regarded as steady at about 100 min within a certain margin of error. Therefore, for sesame oil–water system with poloxamer of 0.35 g/L, the achievement of the steady phase separation probably needs more time according to the above conclusion.

3.3. Corn oil–water emulsions

In contrast to sesame oil–water emulsions, there are predominant and intense oil signals at the top but secondary and weak water signals at the bottom (Fig. 6). Coupled with two photos, we can find that it is different from sesame oil–water systems that there are opaque milky emulsion phase and aqueous phase but not the pure corn oil phase within the whole detection area. Moreover, according to the preliminary inspection, there is also a greater amount of emulsion generated for corn oil–water system with poloxamer 188 of 0.70 g/L than that of 0.35 g/L.

Similar to sesame oil–water systems, oil concentration profiles also experience the process from being mixed to being divided. However, the time scale has changed. In Fig. 6(c), at about 17 min, oil concentrations for upper profiles almost reach maximums. Nevertheless, the process behaves much faster in Fig. 6(f) (at about 5 min). This is in agreement

with the above results for sesame oil–water systems. Slightly different from sesame oil–water systems, oil concentrations at the beginning are not very low. Besides, subsequent oil concentration increases in aqueous phase are not observed, which is probably caused by the decrease in the inhomogeneity of magnetic susceptibility. Further, there are typically two overlapped-profile regions in Fig. 6(c), which are located at the upper part with higher oil concentrations and the nether part with much lower oil concentrations corresponding to the emulsion phase and aqueous phase, respectively. Numbers of profiles between two overlapped-profile regions can be assigned to those voxels located in the transient state. However, there is only one overlapped-profile region located at the upper part corresponding to the emulsion phase (Fig. 6(f)). Other profiles are from those positions at the interface between the emulsion phase and aqueous phase. The absence of the aqueous phase also probably results from a greater amount of emulsion produced as the emulsifier proportion increased.

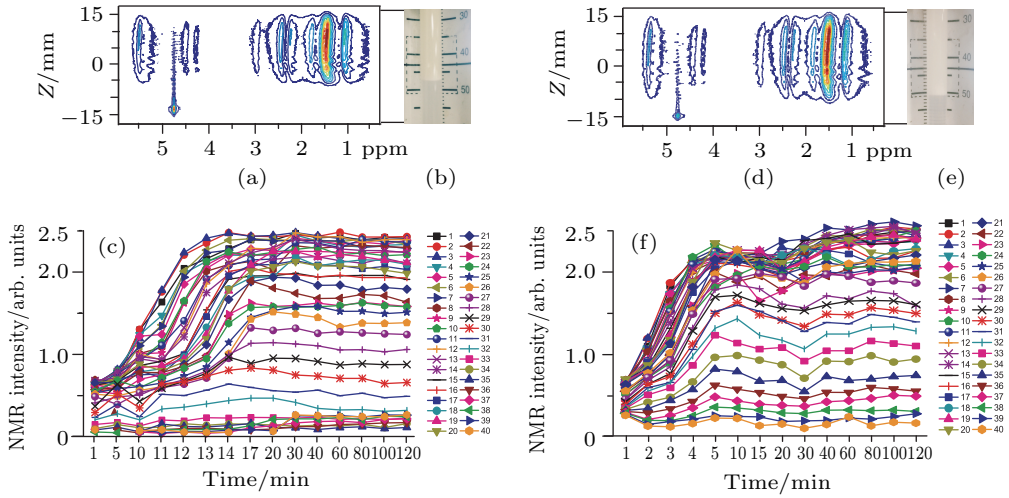


Fig. 6. (color online) Corn oil–water emulsions with 0.35 g/L [(a), (b), and (c)] and 0.70 g/L [(d), (e), and (f)] of poloxamer 188. (a) and (d) 2D chemical shift contours, (b) and (e) sample pictures after 120 min, (c) and (f) evolutions of corn oil profiles versus time.

Besides, unlike sesame oil–water systems with relatively comparable oil and water signal intensities in emulsion phase, corn oil signals in emulsion phases take the predominant roles, but water signals are secondary. We speculate that this results from a big proportion of corn oil being involved in the formation of emulsions compared to sesame oil–water systems. In other words, corn oil tends to be more easily emulsified by poloxamer 188 than sesame oil, which is convinced by the fact that a greater amount of emulsion generates for corn oil systems with the same proportion of emulsifiers. Furthermore, compared to aqueous phases, oil phases are more inclined to separate from emulsion phases for sesame oil–water systems, their concentration profiles jumping to a high level at the beginning of the phase separation. However, for corn oil–water systems, although we cannot examine the separation behavior of the oil phase from the emulsion phase due to its absence in this study, the aqueous phase has been separated from the emulsion phase at the very beginning of the experiment. Due to these different properties, solubilizing excipients formulations based on different water-insoluble lipids (castor oil, olive oil, and sesame oil, etc.) for drug delivery have been developed.[34]

In this article, the feasibility of carrying out spatially resolved spectroscopy and corresponding quantitative analyses of 1D PHASICS have been verified by the application in two kinds of inhomogeneous oil–water emulsion systems. Although the phase separation process observed by NMR experiments on the molecular level can be easily captured by camera, in many cases, however, physical appearances for some objects cannot be distinguished by photos, such as chemical reactions and dynamic processes in transparent solutions. Under such circumstances, the capacity of NMR method would be remarkable. Besides, the performance of PHASICS in a less homogeneous field (i.e., at lower field strength) can be considered from two aspects. On one hand, when the field homogeneity is not good enough, PHASICS probably results in a better result with the improvement of resolution. On the other hand, the SNR of PHASICS at lower field strength is decreased since the sampling mode of EPSI brings more loss of SNR. Therefore, both aspects of resolution and SNR need to be considered to achieve a balanced result. Whereas, with the development of hardware technology including improvement of intensities of pulsed field gradient and magnetic field, the spatial and spectral resolution would be enhanced further.

4. Conclusion

In conclusion, the emulsion formation and subsequent phase separation process for two inhomogeneous oil–water

emulsion systems have been monitored dynamically via 1D PHASICS. With the EPSI detection module, 2D chemical shift contours longitudinally stacked by series of high resolution 1D ^{1}H NMR spectra can be simultaneously recorded by PHASICS both with the chemical shift and spatial information within a few seconds. Compared to single-voxel MRS, multi-voxel spectral information covering the whole effective sample length along the gradient orientation can be accomplished simultaneously. Analyzing 1D spectrum from the most homogeneous detection area, plots of oil concentration profiles versus time and position have been drawn clearly and visually. Furthermore, the phase separation time and emulsion phase length have been determined. For both kinds of emulsion systems, as the emulsifier proportion increased, greater amounts of emulsions are produced and the phase separation process also behaves much faster. However, corn oil exhibits the better emulsifying performance than sesame oil with the emulsifier poloxamer 188. In short, 1D PHASICS is fast and easily implemented, well-resolved, and quantifiable, providing an alternative to research on dynamic processes or chemical reactions.

References

[1] Li Q, Li T, Liu C M, Chen J, Zhang R J, Zhang Z P, Dai T T and McClements D J 2016 *Food Res. Int.* **89** 320

[2] Lobato-Calleros C, Sosa-Perez A, Rodriguez-Tafoya J, Sandoval-Castilla O, Perez-Alonso C and Vemon-Carter E J 2008 *LWT-Food Sci. Technol.* **41** 1847

[3] Relkin P, Shukat R, Peyronel F and Meneau F 2014 *Food Biophys.* **9** 389

[4] Kabri T H, Arab-Tehrany E, Belhaj N and Linder M 2011 *J. Nanobiotechnol.* **9** 41

[5] Nagelreiter C and Valenta C 2013 *Int. J. Pharm.* **456** 517

[6] Onuki Y, Kida C, Funatani C, Hayashi Y and Takayama K 2016 *Int. J. Cosmetic Sci.* **38** 272

[7] Hategekirnana J, Masamba KG, Ma J and Zhong F 2015 *Carbohydr. Polym.* **124** 172

[8] Singh H, Ye A Q and Horne D 2009 *Prog. Lipid Res.* **48** 92

[9] Wanten G J A and Calder P C 2007 *Am. J. Clin. Nutr.* **85** 1171

[10] Warisnoicharoen W, Lansley A B, and Lawrence M J 2000 *Aaps Pharm. Sci.* **2** 16

[11] Huang Z H, Z J J, Ni J, Wang H, Zhao Y 2014 *Chin. Phys. B* **23** 084205

[12] Blonk J C G and Vanaalst H 1993 *Food Res. Int.* **26** 297

[13] Charin R M, Farias A C, Tavares F W and Nele M 2016 *Colloids Surf. Physicochem. Eng. Aspects* **506** 566

[14] Alam M M and Aramaki K 2008 *Langmuir* **24** 12253

[15] Rehage H and Hoffmann H 1991 *Mol. Phys.* **74** 933

[16] Johns M L 2009 *Curr. Opin. Colloid Interface Sci.* **14** 178

[17] Beckonert O, Keun H C, Ebbels T M D, Bundy J G, Holmes E, Lindon J C and Nicholson J K 2007 *Nature Protocols* **2** 2692

[18] Zeng W X, Li Z M and Gao M L 2014 *Acta Phys. Sin.* **63** 018202 (in Chinese)

[19] Vermeir L, Sabatino P, Balcaen M, Declerck A, Dewettinck K, Martins J C, Guthausen G and Van der Meeren P 2016 *J. Colloid Interface Sci.* **475** 57

[20] Jia C H, Shin J A and Lee K T 2015 *J. Agric. Food. Chem.* **63** 10280

[21] Su H Y, Wu C Q, Li D Y and Ai H 2015 *Chin. Phys. B* **24** 017506

[22] Onuki Y, Horita A, Kuribayashi H, Okuno Y, Obata Y and Takayama K 2014 *Drug Dev. Ind. Pharm.* **40** 937

[23] Lambert J, Hergenroder R, Suter D and Deckert V 2009 *Angew. Chem. Int. Ed.* **48** 6343

[24] Mantel C, Bayle P A, Hediger S, Berthon C and Bardet M 2010 *Magn. Reson. Chem.* **48** 600

[25] Martin B T, Chingas G C and McDougal O M 2012 *J. Magn. Reson.* **218** 147

[26] Ke H P, Chen H, Lin Y Q, Wei Z L, Cai S H, Zhang Z Y and Chen Zhong 2014 *Chin. Phys. B* **23** 063201

[27] Wei Z L, Lin L J, Chen Y H, Lin Y Q and Chen Z 2014 *Appl. Phys. Lett.* **105** 132406

[28] Cizauskaite U, Ivanauskas L, Jakštas V, Marksiene R, Jonaitiene L and Bernatoniene J 2016 *Pharm. Dev. Technol.* **21** 716

[29] Opedal N V D T, Sørland G and Sjöblom J 2010 *Energy Fuels* **24** 3628

[30] Saberi A H, Fang Y and McClements D J 2016 *Food Res. Int.* **89** 296

[31] Wu W U, Hettiarachchy N S and Qi M 1998 *J. Am. Oil Chem. Soc.* **75** 845

[32] Borel P, Grolier P, Armand M, Partier A, Lafont H, Lairon D and AzaisBraesco V 1996 *J. Lipid Res.* **37** 250

[33] Cherney D P, Wu C, Thorman R M, Hegner J L, Yeganeh M S, Ferrughelli D and Ulysse E 2015 *Energy Fuels* **29** 3616

[34] Strickley R G 2004 *Pharm. Res.* **21** 201